PHYSICAL REVIEW B **73**, 241403(R) (2006)

Dirac fermion confinement in graphene

N. M. R. Peres,[1] A. H. Castro Neto,[2] and F. Guinea[3]
[1]*Center of Physics and Departamento de Física, Universidade do Minho, P-4710-057, Braga, Portugal*
[2]*Department of Physics, Boston University, 590 Commonwealth Avenue, Boston, Massachusetts 02215, USA*
[3]*Instituto de Ciencia de Materiales de Madrid, CSIC, Cantoblanco E28049 Madrid, Spain*
(Received 4 April 2006; revised manuscript received 7 May 2006; published 15 June 2006)

We study the problem of Dirac fermion confinement in graphene in the presence of a perpendicular magnetic field B. We show, analytically and numerically, that confinement leads to anomalies in the electronic spectrum and to a magnetic-field-dependent crossover from $\sqrt{B}$, characteristic of Dirac-Landau-level behavior, to linear-in-B behavior, characteristic of confinement. This crossover occurs when the radius of the Landau level becomes of the order of the width of the system. As a result, we show that the Shubnikov–de Haas oscillations also change as a function of field, and lead to a singular Landau plot.

DOI: 10.1103/PhysRevB.73.241403 PACS number(s): 81.05.Uw, 71.10.−w, 71.55.−i

The production of two-dimensional (2D) graphene[1,2] and the confirmation, via an anomalous integer quantum Hall effect,[3,4] of the presence of Dirac particles in its electronic spectrum have attracted a great deal of interest. Because of the vanishing of the density of states at the Dirac point, these semimetallic systems present properties that deviate considerably from Landau's Fermi liquid theory.[5,6] In fact, these systems show properties that are similar to models in particle physics and, in particular, to relativistic quantum electrodynamics but with an effective "speed of light" (the Fermi-Dirac velocity v_F) that is substantially smaller than the actual speed of light c ($v_F \approx c/300$). In the most general case, the electron dispersion in graphene can be written in the form of Einstein's equation $E_{\pm}(k)=\pm\sqrt{m^2v_F^4+v_F^2k^2}$, where k is the electron momentum (from now on we use units such that $c=\hbar=1=k_B$) and m is the relativistic mass. In solids this mass represents a gap $\Delta=2mv_F^2$ in the electronic spectrum. This gap can be generated, for instance, by the spin-orbit coupling.[7]

Furthermore, due to experimental constraints, graphene samples are usually mesoscopic in size[8,9] leading to a situation where Dirac fermions are confined by either zigzag or armchair edges to a finite region in space.[10] Confinement is also particularly important for the production of electron waveguides that are the main elements for the production of electronic devices such as all-carbon transistors. Dirac fermion confinement was a particularly enigmatic problem in the early days of quantum mechanics since the formation of wave packets in a region of the size of the Compton wavelength, $\approx 1/m$, requires the use of negative-energy solutions, or antiparticles, the phenomenon called *Zitterbewegung*.[11] Another manifestation of this confinement effect is Klein's paradox where a flux of particles incident on a square potential barrier produces a reflected current that is larger than the incident one. All these effects can manifest themselves when Dirac particles are confined in finite regions of space.

In this paper we show that confinement of Dirac fermions can be studied directly in graphene with the application of a transverse magnetic field. We show that the confinement, generated by the finite size of the sample, shows up in a rather nontrivial way in the electronic spectrum. In particular, we show that the so-called Landau plots (the dependence of electronic spectrum on the magnetic field[12]) is rather nontrivial when the cyclotron length becomes of the order of the size of the sample. We address this problem analytically by studying the Dirac equation in a magnetic field and also by solving numerically the tight-binding model for graphene in a finite geometry.

Graphene is a honeycomb lattice of carbon atoms (with two sublattices A and B) with one electron per π orbital (half-filled band) and can be described by a tight-binding Hamiltonian of the form

$$H_{\mathrm{tb}} = -\sum_{\langle i,j\rangle,\alpha} t_{ij}(a_{i,\alpha}^{\dagger}b_{j,\alpha}+\mathrm{H.c.}), \tag{1}$$

where $a_{i,\alpha}^{\dagger}$ ($a_{i,\alpha}$) creates (annihilates) an electron on site $\mathbf{R}_i$, with spin α ($\alpha=\uparrow,\downarrow$), on sublattice A, $b_{i,\alpha}^{\dagger}$ ($b_{i,\alpha}$) creates (annihilates) an electron on site $\mathbf{R}_i$, with spin α, on sublattice B, $t_{ij}=t\exp\{i\theta_{ij}\}$ is the nearest-neighbor hopping energy ($t\approx 2.7$ eV) in the presence of a magnetic field $\mathbf{B}=B\mathbf{z}$ ($\theta_{ij}=2\pi\int_i^j\mathbf{A}\cdot d\mathbf{l}/\Phi_0$, with $\mathbf{A}=Bx\mathbf{y}$ and $\Phi_0=2\pi/e$ is the quantum of magnetic flux). In the absence of next-nearest-neighbor hopping t' ($\approx 0.1t$), the Hamiltonian is particle-hole symmetric[5] (the Zeeman energy is disregarded).

In a finite system, one has to add the confining potential $H_e=\Sigma_i V_i n_i$, where n_i is the local electronic density. V_i vanishes in the bulk but becomes large at the edge of the sample. We have studied different types of potentials (hard wall, exponential, and parabolic[13]) but in this paper we will focus on a potential that decays exponentially away from the edges into the bulk with a penetration depth λ. In Fig. 1 we show the electronic spectrum for a graphene ribbon of width $L=600a$ ($a=1.42$ Å is the carbon-carbon distance), in the presence of a confining potential $V(x)=V_0(e^{-(x-L/2)/\lambda}+e^{-(L/2-x)/\lambda})$, with strength $V_0=0.1t$ and a penetration depth $\lambda=150a$ (we choose this large value of λ just to illustrate the effect of the confining potential in detail; in real samples we expect $\lambda\approx a$, which is the case discussed in the text), as a function of the momentum k along the ribbon. One can clearly see that in the presence of the confining potential the particle-hole symmetry is broken and, for $V_i>0$, the hole part of the spectrum is strongly distorted. In particular, for k close to the Dirac point, we see that the hole dispersion is

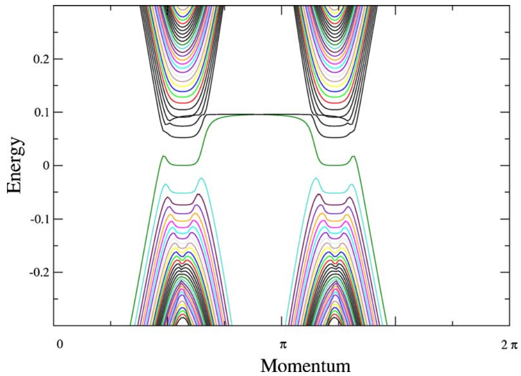

FIG. 1. (Color online) Energy spectrum (in units of t) for a graphene ribbon $600a$ wide, as a function of the momentum k along the ribbon [in units of $1/(\sqrt{3}a)$], with a magnetic flux of $5\times10^{-4}\Phi_0$ per hexagon, in the presence of confining potential (see text).

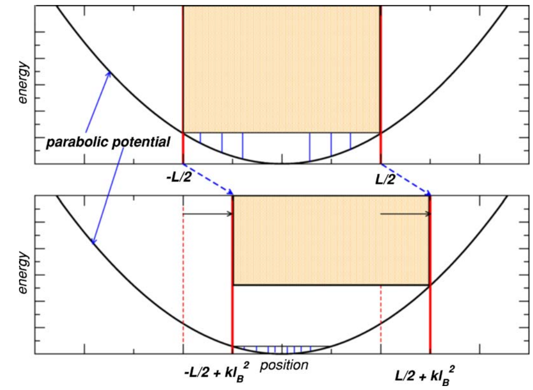

FIG. 2. (Color online) Illustration of the potentials in the problem: $k=0$ (top) and $k\neq0$ (bottom).

given by $E_{n,\sigma=-1}(k)\approx-\gamma_n k^2-\beta_n k^4$ where n is a positive integer, and $\gamma_n<0$ ($\gamma_n>0$) for $n<N^*$ ($n>N^*$). Hence, at $n=N^*$ the hole effective mass *diverges* ($\gamma_{N^*}=0$) and, by tuning the chemical potential μ, via a back gate, to the hole region of the spectrum ($\mu<0$) one should be able to observe an anomaly in the Shubnikov–de Haas (SdH) magnetotransport oscillations. This is how *Zitterbewegung* manifests itself in magnetotransport.

At low energies and long wavelengths, the energy spectrum of Hamiltonian (1) reduces to two Dirac cones centered at the K and K' points in the Brillouin zone. Around each Dirac point the Hamiltonian (1) can be written as

$$H_0=\boldsymbol{\sigma}\cdot(v_F\mathbf{p}+e\mathbf{A}), \tag{2}$$

where $v_F=3ta/2$, $\boldsymbol{\sigma}$ are Pauli matrices acting on the states $\psi(\mathbf{r})=(\psi_A(\mathbf{r}),\psi_B(\mathbf{r}))$ of the two sublattices, and $\mathbf{p}=(p_x,p_y)=-i\boldsymbol{\nabla}$ is the 2D momentum operator. In the absence of confinement $[V(x)=0]$ we can diagonalize (2) and one finds Landau levels given by

$$E_{n,\sigma}=\sigma\sqrt{2}v_F\sqrt{n}/\ell_B=\sigma v_F\sqrt{2eBn}, \tag{3}$$

where $\ell_B=1/\sqrt{eB}$ is the cyclotron length, n is a positive integer (including zero), and $\sigma=1$ (-1) labels the electron (hole) levels.

As discussed in the context of neutrino billiards,[14] the problem in the continuum suffers from the difficulty that in trying to confine massless Dirac particles in a region of size L by including a large potential V at the edge, leads to a situation where particles still exist even at energies higher than V. This problem, of course, does not arise in the tight-binding description. In order to avoid this problem in the continuum description, we introduce a position-dependent mass term $H_c=v_F^2M(x)\sigma_z$, where

$$M(x)=\begin{cases} M, & x<-L/2,\\ 0, & -L/2\le x\le L/2,\\ M, & x>L/2,\end{cases} \tag{4}$$

where L is the width of the graphene stripe. We are interested in the hard wall case ($M\to\infty$) although other potentials can be studied in an analogous way.[13] Notice that in the absence of an applied magnetic field, a mass term does not break particle-hole symmetry, as in the case of a potential $V(x)$.[14] Nevertheless, since both $V(x)$ and $M(x)$ are strongly localized at the edge (in a distance of the order of the lattice spacing), they do not modify the states in the bulk. It is also worth mentioning that although (2) is not time-reversal symmetric in the absence of a magnetic field,[14] time reversal is recovered by the inclusion of the second Dirac cone at the opposite side of the Brillouin zone.

The Dirac equation $H\psi=E\psi$, where $H=H_0+H_c$, can be recast in terms of a wave function ansatz $\phi=(H+E)\psi$ as $H^2\phi=E^2\phi$. It is easy to show that this wave function has the form $\phi(x,y)\propto e^{-iky}\varphi_\sigma(x)$, where k is the momentum along the y direction, $\sigma=\pm1$ are the eigenstates of σ_z, and $\varphi_\sigma(x)$ obeys the following equation:

$$\left(-\frac{\partial^2}{\partial\xi^2}+\xi^2+V(\xi)\right)\varphi_\sigma(\xi)=\epsilon\varphi_\sigma(\xi) \tag{5}$$

where $\xi=x/\ell_B-k\ell_B$, $V(\xi)=[v_F\ell_BM(\xi)]^2$, and $\epsilon=(\ell_BE_\sigma/v_F)^2-\sigma$. Equation (5) is a dimensionless Schrödinger equation for a nonrelativistic particle (of mass 1/2) in a parabolic potential (of frequency $\omega_0=2$) superimposed on a potential well $V(\xi)$, whose position shifts with the momentum k (see Fig. 2). Hence, the Dirac fermion spectrum in the presence of the magnetic field and confining potential is

$$E_{\epsilon,\sigma}=\sigma v_F\sqrt{\epsilon+\sigma}/\ell_B. \tag{6}$$

At low energies (small ϵ) the parabolic potential dominates and the wave functions resemble the ones in the infinite system ($L\to\infty$) in the presence of magnetic field.[5] In this limit, the spectrum of (5) is given by the 1D harmonic oscillator: $\epsilon\approx\omega_0(n+1/2)=2n+1$. This result, together with (6), gives rise to Eq. (3), with the energy proportional to $\sqrt{B}$. On the other hand, at large energies, the confining potential becomes more important and the energy spectrum changes to $\epsilon\approx[\pi n/(L/\ell_B)]^2$, leading to a Dirac fermion spectrum of the form

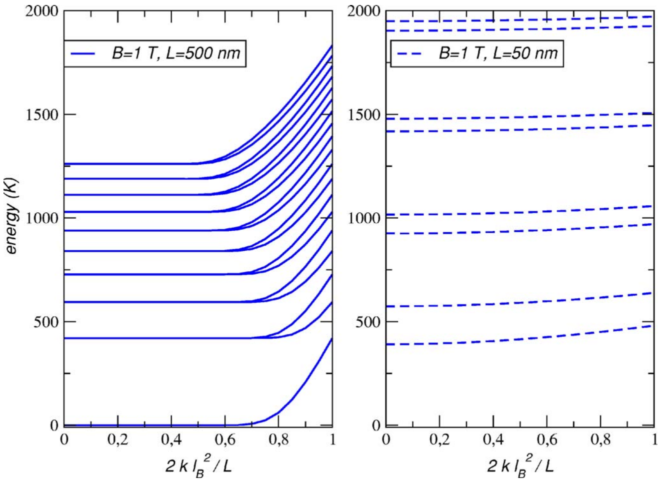

FIG. 3. (Color online) Energy spectrum $E_\sigma(k)$ as function of $k\ell_B^2/L$ for two system sizes $L=50$ and 500 nm, at $B=1$ T, for ten eigenstates. Each Landau level is subdivided into two sublevels, distinguished by the quantum number σ.

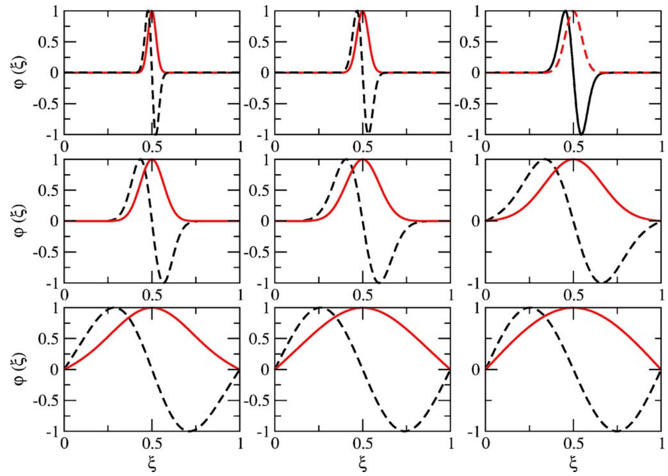

FIG. 4. (Color online) Wave functions φ_σ for $L=500$ nm. The values of the magnetic field are, from left to right and top to bottom, $B=5$, 2.5, 1.25, 0.6, 0.3, 0.1, 0.05, 0.025, 0.01 T.

$$E_{n,\sigma} \approx \sigma v_F[\pi n/L + \sigma LeB/(2\pi n)], \tag{7}$$

which leads to a spectrum proportional to B. These simple arguments show that the SdH magnetoresistance oscillations change behavior as a function of magnetic field. On the one hand, for a given chemical potential μ, Eq. (3) predicts that the maxima of the SdH should happen at fields[15–17]

$$1/B_F(N,L) = (2v_F^2 e/\mu^2)N, \tag{8}$$

where N is the Landau level index. On the other hand, Eq. (7) shows that the maxima occur at fields

$$1/B_F(N,L) = [L^2 e/(2\pi^2 N)]/(N_c(L) - N), \tag{9}$$

where

$$N_c(L) = \mu L/(\pi v_F). \tag{10}$$

Hence, $1/B_F(N)$ *diverges* at a critical Landau level index $N_c(L)$, which increases linearly with the width L of the graphene stripe. The deviation from (8) to (9) is a clear sign of the Dirac fermion confinement.

Notice that the crossover from (3) to (7) [or from (8) to (9)] occurs when the Landau orbit fits into the confining potential. Since each orbit must enclose exactly an integer number of the flux quantum Φ_0, the crossover occurs at a magnetic field B^* such that $B^* L^2 \approx N\Phi_0$, that is,

$$B^*(N,L) = N\Phi_0/L^2. \tag{11}$$

Let us now consider the numerical solution of the differential equation (5) written in terms of the above introduced dimensionless variables in the case $M\to\infty$. Because our treatment of the Dirac equation leads to a second-order differential equation, the appropriate boundary condition for a sharp confining edge with a mass term is[18] $\varphi_\sigma[-L/(2\ell_B)+k\ell_B]=\varphi_\sigma[L/(2\ell_B)+k\ell_B]=0$. In Fig. 3 we show the energy spectrum at $B=1$ T for two different system sizes as a function of $k\ell^2/L$. One can clearly see that the degeneracy of the Landau levels is lifted for small enough system sizes or large enough k.[19,20] For small k the energy states are dispersionless and degenerate.

In Fig. 4 we show the first two state eigenvalues of the effective Schrödinger equation (5), for $k=0$ and different values of the field (or, equivalently, different system sizes). One can clearly observe the change in the wave function from cosine (sine) to Gaussian (first-order Hermite polynomial times Gaussian) behavior as l_B decreases. Clearly the system evolves from a state where the boundaries introduced by the confining potential are irrelevant (the wave functions and the energy levels are essentially those of the 1D harmonic oscillator at $B=5$ T and $l_B \simeq 12$ nm), passing to a state where the Gaussian decay of the wave function in the classically forbidden regions is important, allowing the electrons to experience the presence of the confinement potential (the wave functions and the energy levels cannot be described either by the 1D harmonic oscillator or by the particle in a box for $B=0.1$ T at $l_B \simeq 80$ nm). Finally, when the Landau orbit is of the order of the size of the confinement potential, the eigenstates are essentially those of the particle in a box ($B=0.01$ T, $l_B \simeq 250$ nm).

In Fig. 5, we show the energy spectrum as a function of the magnetic field for different system sizes together with their respective Landau plots. Note that at small fields (when L is large enough) the energy spectrum follows the $\sqrt{B}$ dependence of (3) while at larger fields it becomes linear in B as predicted by (7). The crossover from these two asymptotic behaviors is indeed given by Eq. (11), as one can see from the size dependence. More striking, however, is that fact that $1/B_F$ indeed diverges at sufficiently high Landau level index and that the size dependence is given by (10).

In Fig. 6 we compare our tight-binding results with the experimental data of Ref. 21. We choose a ribbon of size 295 nm (equivalent to $N_c=1197$ unit cells), and Fermi energy $0.069t$ (equivalent to 0.22 eV). Notice the excellent agreement between theory and experiment for $N<16$ ($2<B<10$ T). For $N>16$ there is shift of N by 1 (either plus or minus 1) relative to the experiment. This discrepancy may be associated to the experimental difficulty in assigning the Landau indices at small magnetic fields.[21,22]

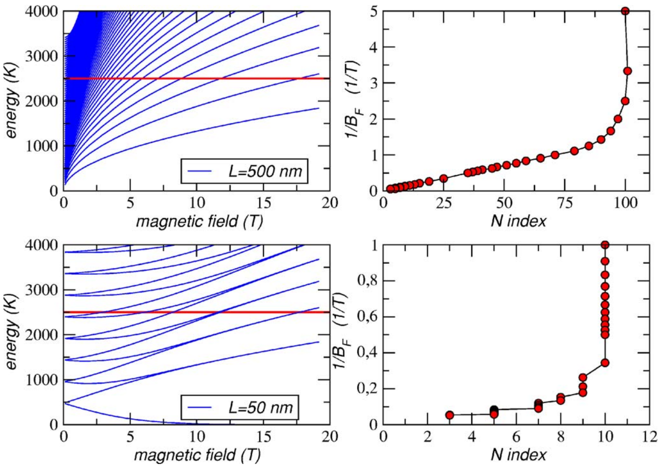

FIG. 5. (Color online) Landau plots for two system sizes L $=500$ and 50 nm. On the right-hand side, we depict the energy levels (in K) as a function of magnetic field (in T) and the horizontal line marks the position of the Fermi energy. On the left-hand side we plot $1/B_F(T)$ as a function of the Landau index N.

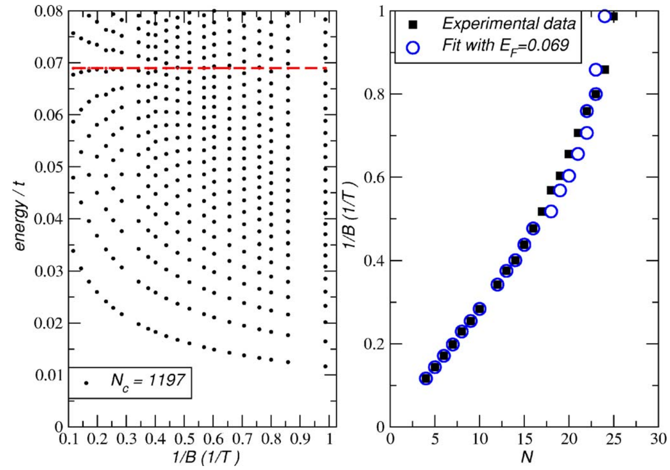

FIG. 6. (Color online) On the left-hand side, we show the energy spectrum (in units of t) as a function of B^{-1} (in T^{-1}). The horizontal line shows the position of the Fermi energy ($\approx 0.069t$). On the right-hand side, we show the theoretical Landau plot (open circles) in comparison with the experiments of Ref. 21 (closed squares).

In summary, we have studied the problem of Dirac confinement in mesoscopic graphene in the presence of a transverse magnetic field. We show that the interplay between size effects and magnetic field can be studied in the continuum limit using the Dirac equation coupled to a vector potential. We present arguments that show that the spectrum of the problem shows a crossover from magnetic field dominated to confinement dominated as a function of magnetic field or system size. The crossover occurs when the radius of the Landau level becomes of the order of the width of the system. In the crossover the spectrum changes from $\sqrt{B}$ to linear in B and that the Landau plots, which can be measured in a SdH experiment, change from dramatically in a finite system.

We are very grateful to C. Berger and W. A. de Heer for providing the experimental data, and A. Geim for many discussions and Ref. 22. A.H.C.N. was supported through NSF Grant No. DMR-0343790. N.M.R.P. thanks ESF Science Programme INSTANS, and FCT under Grant No. POCTI/FIS/58133/2004. F.G. acknowledges funding from MEC (Spain) through Grant No. FIS2005-05478-C02-01.

[1] K. S. Novoselov *et al.*, Science **306**, 666 (2004).
[2] K. S. Novoselov *et al.*, Proc. Natl. Acad. Sci. U.S.A. **102**, 10451 (2005).
[3] K. S. Novoselov *et al.*, Nature (London) **438**, 197 (2005).
[4] Y. Zhang *et al.*, Nature (London) **438**, 201 (2005).
[5] N. M. R. Peres, F. Guinea, and A. H. Castro Neto, Phys. Rev. B **73**, 125411 (2006).
[6] V. M. Pereira, F. Guinea, J. M. B. Lopes dos Santos, N. M. R. Peres, and A. H. Castro Neto, Phys. Rev. Lett. **96**, 036801 (2006).
[7] C. L. Kane and E. J. Mele, Phys. Rev. Lett. **95**, 146802 (2005).
[8] C. Berger *et al.*, J. Phys. Chem. B **108**, 19912 (2004).
[9] Y. Zhang, J. P. Small, M. E. S. Amori, and P. Kim, Phys. Rev. Lett. **94**, 176803 (2005).
[10] N. M. R. Peres, F. Guinea, and A. H. Castro Neto, Phys. Rev. B **73**, 195411 (2006).
[11] C. Itzykson and J. Zuber, *Quantum Field Theory* (McGraw-Hill, New York, 1980).
[12] C. W. J. Beenakker and H. van Houten, Solid State Phys. **44**, 1 (1991).
[13] N. M. R. Peres *et al.* (unpublished).
[14] M. V. Berry and R. J. Mondragon, Proc. R. Soc. London, Ser. A **412**, 53 (1987).
[15] S. G. Sharapov, V. P. Gusynin, and H. Beck, Phys. Rev. B **69**, 075104 (2004).
[16] I. A. Luk'yanchuk and Y. Kopelevich, Phys. Rev. Lett. **93**, 166402 (2004).
[17] V. P. Gusynin and S. G. Sharapov, Phys. Rev. B **71**, 125124 (2005).
[18] E. McCann and V. I. Fal'ko, J. Phys.: Condens. Matter **16**, 2371 (2004).
[19] L. Brey and H. Fertig, cond-mat/0603107 (unpublished).
[20] D. A. Abanin, P. Lee, and L. Levitov, Phys. Rev. Lett. **96**, 176803 (2006).
[21] C. Berger *et al.*, Science **312**, 1191 (2006).
[22] Recently, we received a communication from A. Geim indicating that an alternative description of the data could be made in terms of two types of carriers associated with a bulk multilayer.